Article ID: 1006-8775(2012) 01-0098-10

EVALUATION OF CONVECTIVE-STRATIFORM RAINFALL SEPARATION SCHEMES BY PRECIPITATION AND CLOUD STATISTICS

SHEN Xin-yong (沈新勇)[1], LIU Jia (刘　佳)[1], Xiaofan LI (李小凡)[2]

(1. Key Laboratory of Meteorological Disaster of Ministry of Education, Nanjing University of Information Science and Technology, Nanjing 210044 China; 2. NOAA/NESDIS/Center for Satellite Applications and Research, Camp Springs, Maryland, USA)

Abstract: In this study, two convective-stratiform rainfall partitioning schemes are evaluated using precipitation and cloud statistics for different rainfall types categorized by applying surface rainfall equation on grid-scale data from a two-dimensional cloud-resolving model simulation. One scheme is based on surface rainfall intensity whereas the other is based on cloud content information. The model is largely forced by the large-scale vertical velocity derived from the Tropical Ocean Global Atmosphere Coupled Ocean–Atmosphere Response Experiment (TOGA COARE). The results reveal that over 40% of convective rainfall is associated with water vapor divergence, which primarily comes from the rainfall type with local atmospheric drying and water hydrometeor loss/convergence, caused by precipitation and evaporation of rain. More than 40% of stratiform rainfall is related to water vapor convergence, which largely comes from the rainfall type with local atmospheric moistening and hydrometeor loss/convergence attributable to water clouds through precipitation and the evaporation of rain and ice clouds through the conversion from ice hydrometeor to water hydrometeor. This implies that the separation methods based on surface rainfall and cloud content may not clearly separate convective and stratiform rainfall.

Key words: partitioning scheme; TOGA COARE; convective-stratiform rainfall; statistics

CLC number: P435 **Document code:** A **doi:** 10.3969/j.issn.1006-8775.2012.01.011

1 INTRODUCTION

Convective precipitation is different from stratiform precipitation in four ways. First, convective rain rate is higher than stratiform rain rate. Second, convective rainfall is associated with strong upward motions throughout the troposphere. In contrast, stratiform rainfall is associated with moderate upward motions in the middle and upper troposphere and weak downward motions in the lower troposphere. Third, the horizontal reflectivity gradient over convective regions is stronger than that over stratiform regions. Fourth, the primary microphysical processes that are responsible for the growth of convective and stratiform clouds and precipitation consist of, respectively, the collection of cloud water by rain particles in the strong updraft cores and vapor deposition on ice particles[1]. Furthermore, convective precipitation is dominant during the development of convective systems. When convective systems evolve into the decay stage from the mature phase, deep convective clouds are replaced by anvil clouds and stratiform precipitation becomes dominant.

Due to the nature of available observational and numerical modeling data, the convective-stratiform rainfall separation is based on radar reflectivity or surface rainfall intensity. The assumption that convective cells have peak rainfall rates at least twice as high as the surrounding background rainfall rates has been widely used for decades as the major criterion to identify convective rainfall[2-6]. Other criteria have been used to identify convective and stratiform rainfall, including cloud water and ice and updraft[7-8], liquid water path for stratiform rainfall and cloud water path and rain water path for shallow convection[9], and the fall speed of precipitation particles[10].

As a typical convective-stratiform rainfall separation method, the scheme developed by Tao et al.[11] and modified by Sui et al.[12] (S94) has been

Received 2010-11-11; **Revised** 2011-11-15; **Accepted** 2012-01-15

Foundation item: National Natural Science Foundation of China (41075039, 41175065); National Key Basic Research and Development Project of China (2011CB403405); Chinese Special Scientific Research Project for Public Interest (GYHY200806009); Qinglan Project of Jiangsu Province of China (2009)

Biography: SHEN Xin-yong, Professor, primarily undertaking research on mesoscale meteorology, cloud and precipitation physics.

Corresponding author: SHEN Xin-yong, e-mail: sxydr@126.com

widely used to study convective and stratiform cloud and rainfall processes in two-dimensional (2D) cloud-resolving model frameworks[13-20]. In this scheme, a model grid point is identified as convective if it has a rain rate twice as large as the average rate of the four surrounding grid points (the one grid point on either side of this grid point) and if it has a rain rate of higher than 20 mm h^{-1}. All non-convective cloudy points are categorized as stratiform. Grid points in the stratiform regions are further identified as convective where the cloud water below the melting level is greater than 0.5 g kg^{-1} or where the maximum updraft above 600 hPa exceeds 5 m s^{-1} in raining stratiform regions. Recently, Sui et al.[21] (S07) developed a new convective-stratiform rainfall separation scheme based on cloud content information. In this scheme, the rainfall can be designated convective, mixed, and stratiform when the corresponding range of cloud ratio [the ratio of liquid water path (LWP) to ice water path (IWP)] is smaller than 0.2, between 0.2 and 1.0, and greater than 1, respectively. In addition, grids in raining mixed and stratiform regions whose IWP are larger than 2.55 mm are considered convective.

Lang et al.[10] conducted a comparison study about six separation methods including surface rain rate, mass fluxes, apparent heating and moistening, hydrometeor contents, reflectivity, vertical velocity, microphysics, and latent heat retrieval[2, 5, 7, 9, 10, 22]. They found that the rainfall produced by the method based on surface rain rate is consistently more stratiform whereas the rainfall generated by the new method of Lang et al.[10] was consistently more convective.

Shen et al.[23] studied precipitation and cloud statistics by categorizing the grid-scale simulation data into different rainfall types based on local atmospheric drying / moistening, water vapor convergence/divergence, and hydrometeor loss/gain and hydrometeor convergence/divergence in the surface rainfall budget based on the surface rainfall budget derived by Gao et al.[24] from water vapor and cloud budgets. The separation of rainfall types by Shen et al.[23] is based on physical processes associated with rainfall, whereas the previous convective-stratiform rainfall separation scheme was based on the magnitude of rainfall signal. Rainfall intensity may not be an efficient basis for distinguishing physical processes between rainfalls. In this study, the convective-stratiform rainfall properties partitioned by two convective-stratiform rainfall separation schemes (S94 and S07) will be evaluated using precipitation and cloud statistics for rainfall types proposed by Shen et al.[23]. The model, experiment, and surface rainfall equation and cloud budget are briefly described in section 2. The results are presented in section 3. A summary is given in section 4.

2 MODEL, EXPERIMENT AND BUDGETS

The cloud-resolving model was originally developed by Soong and Ogura[25], Soong and Tao[26], and Tao and Simpson[27]. The two-dimensional version of the model used by Sui et al.[12, 28] and further modified by Li et al.[29, 30] is used in this study. The cloud microphysical parameterization schemes (Table 1) used in the model are from Rutledge and Hobbs[31, 32], Lin et al.[33], Tao et al.[34], and Krueger et al.[35] and the solar and thermal infrared radiation parameterization schemes used in the model are from Chou et al.[36, 37], and Chou and Suarez[38]. The experiment analyzed in this study is conducted using a model forced by zonally uniform vertical velocity, zonal wind, and thermal and moisture advections, which are derived by Professor Minghua Zhang and his research group at the State University of New York at Stony Brook, based on the 6-hourly TOGA COARE observations within the Intensive Flux Array (IFA) region (Zhang, personal communication, 1999). The calculations are based on the application of constrained variational method on column-integrated budgets of mass, heat, moisture, and momentum proposed by Zhang and Lin[39]. Hourly sea surface temperature (SST) at the Improved Meteorological (IMET) surface mooring buoy (1.75° S, 156° E)[40] is also imposed in the model. The model is integrated from 0400 LST 19 December 1992 to 0400 LST 9 January 1993 (A total of 21 days). Fig. 1 shows a time-pressure cross section of the large-scale atmospheric vertical velocity, zonal wind, and the time series of SST during the 21-day period. The horizontal domain is 768 km. A grid mesh of 1.5 km and a time step of 12 seconds are used in the model integrations. A detailed model description can be found in Gao and Li[41]. Hourly grid data are used in the following analysis.

Based on Gao et al.[24] and Cui and Li[13], the surface rain rate (P_S) can be written as

$$P_S = Q_{WVT} + Q_{WVF} + Q_{WVE} + Q_{CM}, \quad (1)$$

where

$$Q_{WVT} = -\frac{\partial [q_v]}{\partial t}, \quad (1a)$$

$$Q_{WVF} = -[\overline{u}^o \frac{\partial \overline{q}_v^{\,o}}{\partial x}] - [\overline{w}^o \frac{\partial \overline{q}_v}{\partial z}] - [\overline{w}^o \frac{\partial q_v^{'}}{\partial z}]$$
$$-[w^{'} \frac{\partial \overline{q}_v}{\partial z}] - [\frac{\partial}{\partial x}(\overline{u}^o + u^{'}) q_v^{'}], \quad (1b)$$

$$Q_{WVE} = \overline{\rho}(w' q_v') |_{z=z_b}, \quad (1c)$$

$$Q_{CM} = -\frac{\partial [q_5]}{\partial t} - [\frac{\partial}{\partial x}(\overline{u}^o q_5)] - [\frac{\partial}{\partial x}(u^{'} q_5)]. \quad (1d)$$

Table 1. List of microphysical processes and parameterization schemes from Rutledge and Hobbs[31] (RH83), 1984 (RH84); Lin et al. 1983 (LFO), Tao et al. 1989 (TSM) and Krueger et al. 1995 (KFLC).

Notation	Description	Scheme
P_{MLTG}	Growth of vapor by evaporation of liquid from graupel surface	RH84
PMLTS	Growth of vapor by evaporation of melting snow	RH83
PREVP	Growth of vapor by evaporation of raindrops	RH83
PIMLT	Growth of cloud water by melting of cloud ice	RH83
PCND	Growth of cloud water by condensation of supersaturated vapor	TSM
PGMLT	Growth of raindrops by melting of graupel	RH84
PSMLT	Growth of raindrops by melting of snow	RH83
PRACI	Growth of raindrops by the accretion of cloud ice	RH84
PRACW	Growth of raindrops by the collection of cloud water	RH83
PRACS	Growth of raindrops by the accretion of snow	RH84
PRAUT	Growth of raindrops by the autoconversion of cloud water	LFO
PIDW	Growth of cloud ice by the deposition of cloud water	KFLC
PIACR	Growth of cloud ice by the accretion of rain	RH84
PIHOM	Growth of cloud ice by the homogeneous freezing of cloud water	
PDEP	Growth of cloud ice by the deposition of supersaturated vapor	TSM
PSAUT	Growth of snow by the conversion of cloud ice	RH83
PSACI	Growth of snow by the collection of cloud ice	RH83
PSACW	Growth of snow by the accretion of cloud water	RH83
PSFW	Growth of snow by the deposition of cloud water	KFLC
PSFI	Depositional growth of snow from cloud ice	KFLC
PSACR	Growth of snow by the accretion of raindrops	LFO
PSDEP	Growth of snow by the deposition of vapor	RH83
PGACI	Growth of graupel by the collection of cloud ice	RH84
PGACR	Growth of graupel by the accretion of raindrops	RH84
PGACS	Growth of graupel by the accretion of snow	RH84
PGACW	Growth of graupel by the accretion of cloud water	RH84
PWACS	Growth of graupel by the riming of snow	RH84
PGDEP	Growth of graupel by the deposition of vapor	RH84
PGFR	Growth of graupel by the freezing of raindrops	LFO

Here, q_v is specific humidity; u and w are the zonal and vertical components of wind, respectively; $\overline{\rho}$ is height dependent mean air density; $q_5 = q_2 + q_3$, $q_2 = q_c + q_r$, $q_3 = q_i + q_s + q_g$, where q_c, q_r, q_i, q_s, q_g are the mixing ratios of cloud water, raindrops, cloud ice, snow, and graupel, respectively; overbar denotes a model domain mean; prime is a perturbation from model domain mean; $[()](=\int_{z_b}^{z_t}\overline{\rho}()dz)$ is mass integration, and z_t and z_b are the heights of the top and bottom of the model atmosphere respectively; and superscript ° is an imposed COARE-observed value. In Eq. (1), Q_{WVT}, Q_{WVF}, Q_{WVE}, and Q_{CM} denote local water vapor change, water vapor convergence, surface evaporation, and hydrometeor change/convergence, respectively. Whereas Q_{WVT}, Q_{WVF}, and Q_{CM} could be positive or negative, Q_{WVE} is positive.

Hydrometeor change/convergence (Q_{CM}) are from water (Q_{CMW}) and ice (Q_{CMI}) clouds. Following Sui and Li[42], the cloud budget can be written as

$$Q_{CM} = Q_{CMI} + Q_{CMW}, \quad (2)$$

$$Q_{CMI} = -P_{DEP} - P_{SDEP} - P_{GDEP} + C(IWP, LWP) + P_{MLTS} + P_{MLTG}, \quad (2a)$$

$$P_{CMW} = P_S - P_{CND} - C(IWP, LWP) + P_{REVP}, \quad (2b)$$

where

$$Q_{CMI} = -\frac{\partial[q_3]}{\partial t} - [\frac{\partial}{\partial x}(\overline{u}^o q_3)] - [\frac{\partial}{\partial x}(u' q_3)], \quad (2c)$$

$$Q_{CMW} = -\frac{\partial[q_2]}{\partial t} - [\frac{\partial}{\partial x}(\overline{u}^o q_2)] - [\frac{\partial}{\partial x}(u' q_2)], \quad (2d)$$

$$C(IWP,LWP) = -P_{SACW}(T<T_o) - P_{SFW}(T<T_o) - P_{GACW}(T<T_o) - P_{IHOM}(T<T_{oo}) + P_{IMLT}(T>T_o) - P_{IDW}(T_{oo}<T<T_o) + P_{RACS}(T<T_o) - P_{IACR}(T<T_o) - P_{GACR}(T<T_o) - P_{SACR}(T<T_o) - P_{GFR}(T<T_o) + P_{SMLT}(T>T_o) + P_{GMLT}(T>T_o). \quad (2e)$$

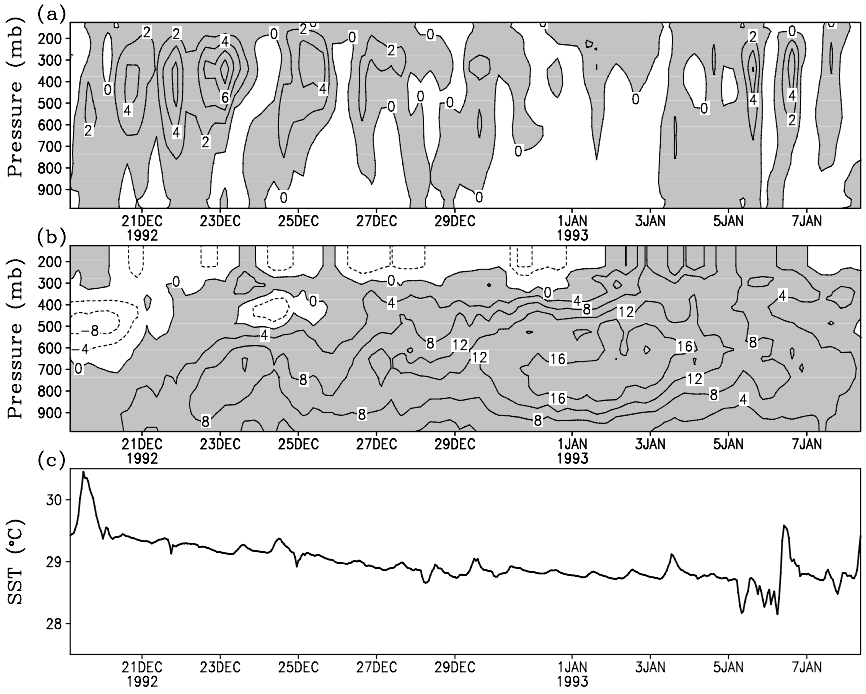

Figure 1. Time-pressure cross section of (a) vertical velocity (cm s-1), (b) zonal wind (m s-1), and the time series of (c) sea surface temperature (°C) derived from observations made in TOGA COARE for 21-day period. Upward motion in (a) and westerly wind in (b) are shaded.

Here, Eqs. (2a) and (2b) are water and ice cloud budgets, respectively. Ice water path (IWP) is the sum of mass integrations of mixing ratios of cloud water and raindrops, and liquid water path (LWP) is the sum of mass integrations of mixing ratios of cloud ice, snow, and graupel. Eq. (2e) is the conversion between the ice and water hydrometeors, which is mainly caused by the accretion of cloud water by precipitation hydrometeors (P_{SACW} + P_{GACW}) and the melting of precipitation hydrometeors to rain (P_{SMLT} + P_{GMLT}) in the deep tropical convective regime[30]. Cloud microphysical processes and their parameterization schemes in Eq. (2) can be found in Table 1.

Following Shen et al.[23], *T* and *t* represent local atmospheric drying (Q_{WVT} >0) and moistening (Q_{WVT} <0), respectively. *F* and *f* denote water vapor convergence (Q_{WVF} >0) and divergence (Q_{WVF} <0), respectively. *M* and *m* represent hydrometeor loss/convergence (Q_{CM} >0) and hydrometeor gain/divergence (Q_{CM} <0), respectively. Thus, seven rainfall types (TFM, TFm, tFM, tFm, TfM, Tfm, tfM) will be calculated using grid-scale data and analyzed in this study (see the summary of rainfall types in Table 2). Because the rainfall type tfm makes a negligibly small contribution to total rainfall, it is not discussed in section 3.

3 RESULTS

The analysis of surface rainfall budgets averaged for stratiform and convective rainfall partitioned using the S94 method in Table 3a shows that stratiform rainfall is associated with local atmospheric drying and hydrometeor loss/convergence and surface evaporation while water vapor divergence prevails over raining stratiform regions. The convective rainfall is primarily related to the local atmospheric drying and water vapor convergence while hydrometeor gain/divergence occurs over convective regions. The stratiform rainfall shows similar

magnitudes of IWP (Table 4a), whereas the LWP is over three times larger than the IWP over convective regions. One-third and two-thirds of hydrometeor loss/convergence over raining stratiform regions are from ice and water clouds respectively. The water hydrometeor loss/convergence results from precipitation and evaporation of rain, whose rates are larger than the vapor condensation rate and the conversion rate from ice hydrometeor to water hydrometeor. The ice hydrometeor loss/convergence is attributable to the conversion from ice hydrometeor to water hydrometeor. Over convective regions, 40% and 60% of hydrometeor gain/divergence are, respectively, from ice and water clouds. The water hydrometeor gain/divergence is primarily caused by vapor condensation, which is larger than the surface rainfall, whereas vapor depositions cause ice hydrometeor gain/divergence.

Table 2. Summary of rainfall types. T and t represent local atmospheric drying and moistening, respectively. F and f represent water vapor convergence and divergence, respectively. M and m represent hydrometeor loss/convergence and gain/divergence, respectively.

Type	Description
TFM	Water vapor convergence, local atmospheric drying, and hydrometeor loss/convergence
TFm	Water vapor convergence, local atmospheric drying, and hydrometeor gain/divergence
tFM	Water vapor convergence, local atmospheric moistening, and hydrometeor loss/convergence
tFm	Water vapor convergence, local atmospheric moistening, and hydrometeor gain/divergence
TfM	Water vapor divergence, local atmospheric drying, and hydrometeor loss/convergence
Tfm	Water vapor divergence, local atmospheric drying, and hydrometeor gain/divergence
tfM	Water vapor divergence, local atmospheric moistening, and hydrometeor loss/convergence
tfm	Water vapor divergence, local atmospheric moistening, and hydrometeor gain/divergence

Table 3. Means of P_S, Q_{WVT}, Q_{WVF}, Q_{WVE}, and Q_{CM} for (a) stratiform and convective rainfall partitioned using the S94 method and (b) stratiform, mixed, and convective rainfall partitioned using the S07 method. Units are mm h^{-1}

(a)	Stratiform rainfall	Convective rainfall
P_S	1.43	10.47
Q_{WVT}	1.12	5.88
Q_{WVF}	–1.20	8.88
Q_{WVE}	0.24	0.43
Q_{CM}	1.26	–4.72

(b)	Stratiform rainfall	Mixed rainfall	Convective rainfall
P_S	0.40	2.59	6.93
Q_{WVT}	0.95	1.36	3.95
Q_{WVF}	–1.57	–1.04	5.04
Q_{WVE}	0.21	0.26	0.37
Q_{CM}	0.82	2.01	–2.43

Table 4. Means of *IWP*, *LWP*, Q_{CM}, Q_{CMI}, Q_{CMW}, P_S, $-P_{CND}$, $-(P_{DEP}+P_{SDEP}+P_{GDEP})$, P_{REVP}, $P_{MLTS}+P_{MLTG}$, and *C(LWP, IWP)* for (a) stratiform and convective rainfall partitioned using the S94 method and (b) stratiform, mixed, and convective rainfall partitioned using the S07 method. Units are mm for *IWP* and *LWP* and mm h^{-1} for the others.

(a)	Stratiform rainfall	Convective rainfall
IWP	0.79	1.09
LWP	0.83	3.55
Q_{CM}	1.26	–4.72
Q_{CMI}	0.43	–1.88
Q_{CMW}	0.83	–2.84
P_S	1.43	10.47
$-P_{CND}$	–1.11	–15.82
$-(P_{DEP}+P_{SDEP}+P_{GDEP})$	–0.63	–1.30
P_{REVP}	1.52	1.87
$(P_{MLTS}+P_{MLTG})$	0.06	0.07
C(IWP, LWP)	1.01	–0.65

(b)	Stratiform rainfall	Mixed rainfall	Convective rainfall
IWP	0.75	0.52	1.24
LWP	0.35	1.14	2.71
Q_{CM}	0.82	2.01	–2.43
Q_{CMI}	0.33	0.43	–0.84
Q_{CMW}	0.48	1.57	–1.59
P_S	0.40	2.59	6.93
$-P_{CND}$	–0.11	–1.88	–10.28
$-(P_{DEP}+P_{SDEP}+P_{GDEP})$	–0.64	–0.35	–1.25
P_{REVP}	1.11	1.62	2.07
$(P_{MLTS}+P_{MLTG})$	0.05	0.02	0.10
C(IWP, LWP)	0.92	0.76	0.31

The calculation in S07 (Table 3b) reveals that the stratiform and convective rainfall budgets are similar to those in S94 but the magnitudes in S07 are generally smaller than those in S94. The mixed rainfall budget is similar to the stratiform rainfall budget. The similarities in cloud budgets between S07 and S94 show that the IWP is smaller than the LWP over convective regions and that similar vapor deposition rates and conversion rate from ice clouds to water clouds lead to similar ice cloud budgets over raining stratiform regions. The differences in cloud budgets between S07 and S94 include the following: (1) over raining stratiform regions, the IWP is significantly larger than the LWP in S07 whereas they

are similar in S94; (2) the evaporation rate of rain is much larger than the stratiform rain rate and becomes the primary process in the water hydrometeor loss/convergence in S07, whereas they contribute equally to the water hydrometeor loss/convergence in S94; (3) ice hydrometeor concentration is converted to water hydrometeor concentration in S07, whereas water hydrometeor is converted to ice hydrometeor in S94. The IWP is smaller than the LWP over mixed rainfall regions, which is similar to that over convective regions. The hydrometeor loss/convergence over mixed rainfall regions comes primarily from water clouds, caused by precipitation and evaporation of rain.

To evaluate rainfall partitioning methods, we analyze rainfall and cloud statistics for each rainfall region by calculating fractional rainfall coverage (FRC) and percentage of rain amount over total rainfall amount (PRA) and surface rainfall and cloud budgets. Over raining stratiform regions in S94, rainfall with local atmospheric drying and water vapor divergence and hydrometeor loss/convergence (TfM; 41.22%) makes the largest contribution to stratiform rainfall, and occupies 37.44% of stratiform rainfall areas (Table 5a). The local atmospheric drying rate, which is from the water vapor divergence, is three times larger than the rate of hydrometeor loss/convergence. Thus, the hydrometeor loss/convergence plays an important role in producing rainfall in TfM. The IWP and LWP of TfM have similar magnitudes (Table 6a). In TfM (Table 6a) and stratiform rainfall (Table 4a), 34.1% and 65.9% of hydrometeor loss/convergence of TfM come, respectively, from ice and water clouds. The cloud budgets of TfM are similar to those averaged for stratiform rainfall, but the magnitudes of the former are generally smaller than those of the latter. 47.73% of stratiform rainfall is attributable to rainfall types with water vapor convergence, which comes primarily from the rainfall type with local atmospheric moistening, water vapor convergence, and hydrometeor loss/convergence (tFM; 26.93%) due to large surface rainfall (0.38 mm h^{-1}) and coverage (27.38%) (Table 5a). Water vapor convergence mainly moistens the local atmosphere whereas surface rainfall corresponds to the hydrometeor loss/convergence. All rainfall types have similar magnitudes for the IWP and LWP (Table 6a).

Table 5. Fractional rainfall coverage (*FRC*), percentage of rain amount over total rainfall amount (*PRA*), and means of P_S, Q_{WVT}, Q_{WVF}, Q_{WVE}, and Q_{CM} in TFM, TFm, tFM, tFm, TfM, Tfm, and tfM for (a) stratiform rainfall and (b) convective rainfall partitioned using the S94 method. Units are mm h^{-1} for P_S, Q_{WVT}, Q_{WVF}, Q_{WVE}, and Q_{CM} and % for *FRC* and *PRA*.

(a)	**TFM**	**TFm**	**tFM**	**tFm**	**TfM**	**Tfm**	**tfM**
FRC	0.42	4.74	27.38	12.47	37.44	10.82	6.71
PRA	2.80	8.38	26.93	9.62	41.22	5.01	6.04
P_S	0.04	0.12	0.38	0.14	0.59	0.07	0.09
Q_{WVT}	0.01	0.18	–2.57	–1.03	3.64	1.00	–0.11
Q_{WVF}	0.01	0.25	2.18	1.61	–4.41	–0.72	–0.12
Q_{WVE}	0.00	0.01	0.06	0.03	0.09	0.03	0.02
Q_{CM}	0.02	–0.32	0.71	–0.46	1.26	–0.23	0.30

(b)	**TFM**	**TFm**	**tFM**	tFm	**TfM**	**Tfm**	**tfM**
FRC	4.10	15.64	13.84	27.11	26.54	10.23	2.52
PRA	13.82	22.71	15.11	16.65	25.28	5.01	1.41
P_S	1.45	2.38	1.58	1.74	2.65	0.52	0.15
Q_{WVT}	0.39	2.09	–2.41	–5.19	8.26	2.82	–0.08
Q_{WVF}	0.50	4.30	2.79	11.95	–8.96	–1.56	–0.13
Q_{WVE}	0.02	0.08	0.06	0.12	0.10	0.05	0.01
Q_{CM}	0.54	–4.08	1.15	–5.13	3.24	–0.78	0.35

Over convective regions in S94, the largest contributors to convective rainfall are TfM (25.28%) and the rainfall type with local atmospheric drying, water vapor convergence, and hydrometeor gain/divergence (TFm; 22.71%) due to large surface rain rates for TfM (2.65 mm h^{-1}) and TFm (2.38 mm h^{-1}) and large rainfall coverage (26.54%) for TfM (Table 5b). In TfM, water vapor divergence mainly dries the local atmosphere whereas hydrometeor loss/convergence is responsible for surface rainfall. Water vapor convergence balances out the hydrometeor gain/divergence and surface rainfall leads to local atmospheric drying in TFm. The LWP is larger than the IWP in TfM and TFm (Table 6b). The hydrometeor loss/convergence in TfM is caused by water clouds due to precipitation. The hydrometeor gain/divergence in TFm is attributable to water clouds through vapor condensation and to ice clouds through vapor depositions and the conversion from water hydrometeor to ice hydrometeor. 68.29% of convective rainfall comes from rainfall types with water vapor convergence, which cover 60.69% of convective rainfall areas (Table 5b). The LWP is much larger than the IWP and the hydrometeor change/convergence results largely from water clouds depending on the relative importance of precipitation

and vapor condensation (Table 6b).

Table 6. Means of IWP, LWP, QCM, QCMI, QCMW, PS, -PCND, -(PDEP+PSDEP+PGDEP), PREVP, PMLTS+PMLTG, and C(LWP, IWP) in TFM, TFm, tFM, tFm, TfM, Tfm, tfM, and tfm for (a) stratiform rainfall and (b) convective rainfall partitioned using the S94 method. Units are mm for IWP and LWP and mm h^{-1} for the others.

(a)	TFM	TFm	tFM	tFm	TfM	Tfm	tfM
IWP	0.01	0.08	0.18	0.12	0.26	0.09	0.06
LWP	0.01	0.09	0.18	0.14	0.28	0.09	0.05
Q_{CM}	0.02	–0.32	0.71	–0.46	1.26	–0.23	0.30
Q_{CMI}	0.00	–0.13	0.19	–0.09	0.43	–0.06	0.10
Q_{CMW}	0.02	–0.19	0.52	–0.37	0.83	–0.18	0.20
P_S	0.04	0.12	0.38	0.14	0.59	0.07	0.09
$-P_{CND}$	–0.03	–0.43	0.06	–0.59	0.10	–0.31	0.09
$-(P_{DEP}+P_{SDEP}+P_{GDEP})$	–0.01	–0.11	–0.09	–0.15	–0.12	–0.14	–0.02
P_{REVP}	0.01	0.09	0.35	0.14	0.66	0.14	0.13
$(P_{MLTS}+P_{MLTG})$	0.00	0.00	0.01	0.00	0.03	0.00	0.01
C(IWP, LWP)	0.01	–0.03	0.27	0.05	0.52	0.07	0.10

(b)	TFM	TFm	tFM	tFm	TfM	Tfm	tfM
IWP	0.05	0.29	0.12	0.23	0.25	0.14	0.02
LWP	0.27	0.97	0.37	0.99	0.61	0.29	0.04
Q_{CM}	0.54	–4.08	1.15	–5.13	3.24	–0.78	0.35
Q_{CMI}	–0.03	–1.34	0.09	–0.64	0.28	–0.27	0.03
Q_{CMW}	0.57	–2.75	1.06	–4.49	2.96	–0.52	0.32
P_S	1.45	2.38	1.58	1.74	2.65	0.52	0.15
$-P_{CND}$	–1.01	–6.33	–0.60	–6.84	0.10	–1.30	0.15
$-(P_{DEP}+P_{SDEP}+P_{GDEP})$	–0.04	–0.50	–0.07	–0.30	–0.17	–0.22	–0.01
P_{REVP}	0.14	0.36	0.23	0.26	0.63	0.20	0.06
$(P_{MLTS}+P_{MLTG})$	0.00	0.01	0.01	0.01	0.03	0.01	0.00
C(IWP, LWP)	0.01	–0.85	0.15	–0.35	0.42	–0.06	0.04

Over raining stratiform regions in S07, the total rainfall consists largely of the rainfall types TfM (44.13%) and tFM (28.3%) due to large stratiform rainfall coverage and a relatively high rain rate (Table 7a). The local atmospheric drying is offset by the water vapor divergence in TfM whereas the local atmospheric moistening is largely balanced out by the water vapor convergence in tFM. As a result, hydrometeor loss/convergence plays an important role in the surface rainfall budget. The IWP is twice as large as the LWP (Table 8a). The hydrometeor loss/convergence is caused by water clouds through the evaporation of rain and ice clouds through its conversion to water hydrometeor.

Over convective regions in S07, rainfall types TfM (26.03%) and TFm (21.97%) contribute to total rainfall through the high rain rate for both rainfall types and the large convective rainfall coverage for TfM (Table 7c). Water vapor divergence dries the local atmosphere and the convective rainfall largely corresponds to the hydrometeor loss/convergence in TfM. Hydrometeor gain/divergence nearly balances out water vapor convergence and convective rainfall is attributable to the local atmospheric drying in TFm. The hydrometeor loss/convergence in TfM is caused by water clouds through precipitation and the evaporation of rain (Table 8c). The hydrometeor gain/divergence in TFm is caused by water clouds through vapor condensation and by ice clouds through vapor depositions and the conversion from water hydrometeor to ice hydrometeor.

The precipitation statistics over mixed rainfall regions are similar to those over raining stratiform regions, in which total rainfall consists largely of the rainfall types TfM (43.51%) and tFM (24.49%) (Table 7b). Unlike the cloud statistics over raining stratiform regions, the cloud statistics over mixed rainfall regions show that water clouds and microphysical processes play more important roles than ice clouds do (Table 8b). The LWP is twice as large as the IWP. Hydrometeor loss/convergence is mainly caused by precipitation and the evaporation of rain.

Table 7. Fractional rainfall coverage (*FRC*), percentage of rain amount over total rainfall amount (*PRA*), and means of P_S, Q_{WVT}, Q_{WVF}, Q_{WVE}, and Q_{CM} in TFM, TFm, tFM, tFm, TfM, Tfm, tfM, and tfm for (a) stratiform rainfall and (b) mixed rainfall and (c) convective rainfall partitioned using the S07 method. Units are mm h^{-1} for P_S, Q_{WVT}, Q_{WVF}, Q_{WVE}, and Q_{CM} and % for *FRC* and *PRA*.

(a)	TFM	TFm	tFM	tFm	TfM	Tfm	tfM
FRC	0.06	3.89	29.30	11.16	35.83	12.40	7.34
PRA	0.32	3.14	28.30	7.90	44.13	8.27	7.94
P_S	0.00	0.01	0.11	0.03	0.18	0.03	0.03
Q_{WVT}	0.00	0.07	–2.21	–0.63	2.88	0.93	–0.09
Q_{WVF}	0.00	0.06	1.79	0.83	–3.46	–0.70	–0.10
Q_{WVE}	0.00	0.01	0.06	0.02	0.08	0.03	0.02
Q_{CM}	0.00	–0.13	0.48	–0.19	0.67	–0.23	0.21

(b)	TFM	TFm	tFM	tFm	TfM	Tfm	tfM
FRC	0.82	4.16	27.56	12.47	40.75	7.84	6.38
PRA	4.75	7.04	24.49	10.78	43.51	3.46	5.96
P_S	0.12	0.18	0.63	0.28	1.13	0.09	0.15
Q_{WVT}	0.03	0.22	–2.95	–1.35	4.68	0.82	–0.11
Q_{WVF}	0.04	0.30	2.60	2.33	–5.61	–0.57	–0.13
Q_{WVE}	0.00	0.01	0.07	0.03	0.11	0.02	0.02
Q_{CM}	0.04	–0.35	0.92	–0.74	1.94	–0.19	0.38

(c)	TFM	TFm	tFM	tFm	TfM	Tfm	tfM
FRC	2.66	12.58	17.30	22.42	30.30	11.04	3.69
PRA	12.21	21.97	17.03	15.66	26.03	5.29	1.80
P_S	0.85	1.52	1.18	1.09	1.80	0.37	0.12
Q_{WVT}	0.23	1.40	–2.59	–3.67	6.39	2.29	–0.10
Q_{WVF}	0.28	2.81	2.66	7.97	–7.17	–1.36	–0.14
Q_{WVE}	0.01	0.06	0.06	0.09	0.10	0.04	0.01
Q_{CM}	0.32	–2.74	1.05	–3.30	2.49	–0.60	0.36

Table 8. Means of *IWP*, *LWP*, Q_{CM}, Q_{CMI}, Q_{CMW}, P_S, $-P_{CND}$, $-(P_{DEP}+P_{SDEP}+P_{GDEP})$, P_{REVP}, $P_{MLTS}+P_{MLTG}$, and *C(LWP, IWP)* in TFM, TFm, tFM, tFm, TfM, Tfm, tfM, and tfm for (a) stratiform rainfall and (b) mixed rainfall and (c) convective rainfall partitioned using the S07 method. Units are mm for *IWP* and *LWP* and mm h^{-1} for the others.

(a)	TFM	TFm	tFM	tFm	TfM	Tfm	tfM
IWP	0.00	0.04	0.19	0.11	0.24	0.11	0.06
LWP	0.00	0.02	0.09	0.05	0.12	0.05	0.03
Q_{CM}	0.00	–0.13	0.48	–0.19	0.67	–0.23	0.21
Q_{CMI}	0.00	–0.04	0.16	–0.06	0.28	–0.08	0.07
Q_{CMW}	0.00	–0.09	0.32	–0.13	0.40	–0.15	0.14
P_S	0.00	0.01	0.11	0.03	0.18	0.03	0.03
$-P_{CND}$	0.00	–0.11	0.17	–0.18	0.14	–0.21	0.08
$-(P_{DEP}+P_{SDEP}+P_{GDEP})$	0.00	–0.08	–0.10	–0.15	–0.11	–0.19	–0.02
P_{REVP}	0.00	0.04	0.28	0.11	0.44	0.13	0.11
$(P_{MLTS}+P_{MLTG})$	0.00	0.00	0.01	0.00	0.03	0.00	0.00
C(IWP, LWP)	0.00	0.04	0.24	0.09	0.36	0.11	0.09

(b)	TFM	TFm	tFM	tFm	TfM	Tfm	tfM
IWP	0.01	0.04	0.12	0.08	0.19	0.04	0.03
LWP	0.03	0.11	0.24	0.20	0.41	0.09	0.06
Q_{CM}	0.04	–0.35	0.92	–0.74	1.94	–0.19	0.38
Q_{CMI}	0.00	–0.11	0.20	–0.08	0.40	–0.05	0.08
Q_{CMW}	0.04	–0.24	0.72	–0.66	1.54	–0.13	0.30
P_S	0.12	0.18	0.63	0.28	1.13	0.09	0.15
$-P_{CND}$	–0.10	–0.55	–0.05	–1.06	0.12	–0.33	0.09
$-(P_{DEP}+P_{SDEP}+P_{GDEP})$	–0.01	–0.05	–0.06	–0.08	–0.09	–0.05	–0.01
P_{REVP}	0.02	0.07	0.39	0.12	0.77	0.10	0.14
$(P_{MLTS}+P_{MLTG})$	0.00	0.00	0.01	0.00	0.01	0.00	0.00
C(IWP, LWP)	0.01	–0.06	0.26	0.00	0.48	0.00	0.09

(c)	TFM	TFm	tFM	tFm	TfM	Tfm	tfM
IWP	0.04	0.27	0.17	0.23	0.33	0.15	0.05
LWP	0.16	0.68	0.34	0.69	0.54	0.25	0.05
Q_{CM}	0.32	–2.74	1.05	–3.30	2.49	–0.60	0.36
Q_{CMI}	–0.01	–0.97	0.16	–0.47	0.52	–0.16	0.10
Q_{CMW}	0.34	–1.78	0.89	–2.83	1.97	–0.44	0.26
P_S	0.85	1.52	1.18	1.09	1.80	0.37	0.12
$-P_{CND}$	–0.59	–4.17	–0.36	–4.35	0.04	–0.99	0.13
$-(P_{DEP}+P_{SDEP}+P_{GDEP})$	–0.03	–0.42	–0.10	–0.30	–0.18	–0.20	–0.01
P_{REVP}	0.09	0.31	0.31	0.26	0.78	0.21	0.10
$(P_{MLTS}+P_{MLTG})$	0.00	0.01	0.01	0.01	0.05	0.01	0.01
C(IWP, LWP)	0.02	–0.55	0.24	–0.18	0.65	0.03	0.10

4 SUMMARY

Two convective-stratiform rainfall separation schemes are evaluated using the precipitation and cloud statistics for seven rainfall types in this study. One scheme (S94), developed by Tao et al.[11] and modified by Sui et al.[12], was based on surface rainfall intensity, whereas the other (S07), developed by Sui et al.[21], was based on the ratio of liquid water path to ice water path (cloud ratio). The grid-scale data used in this study is from a two-dimensional cloud resolving model simulation that is imposed by the forcing from the Tropical Ocean Global Atmosphere Coupled Ocean–Atmosphere Response Experiment (TOGA COARE). The rainfall types are categorized based on different surface rainfall processes including local atmospheric drying/moistening, water vapor convergence/divergence, and hydrometeor loss/gain and hydrometeor convergence/ divergence proposed by Gao et al.[24]. The results show that the rainfall types with water vapor divergence and convergence make significant contributions to convective and stratiform rainfall, respectively. 31.7% of convective rainfall comes from the rainfall types with water vapor divergence whereas 47.7% of stratiform rainfall comes from rainfall types with water vapor convergence in S94. 39.7% of convective rainfall comes from rainfall types with water vapor divergence whereas 33.1% of stratiform rainfall comes from rainfall types with water vapor convergence in S07. This indicates that surface rainfall intensity and the cloud ratio cannot exclude the rainfall types with water vapor divergence from convective rainfall and the rainfall types with water vapor convergence from stratiform rainfall. The analysis of convective-stratiform rainfall may contain great uncertainty, in particular, in the analysis of stratiform rainfall where nearly half of stratiform rainfall is associated with water vapor convergence.

Convective rainfall is mainly attributable to the rainfall types with local atmospheric drying, water vapor divergence, and hydrometeor loss/convergence (TfM) and local atmospheric drying, water vapor convergence, and hydrometeor gain/divergence (TFm) whereas stratiform rainfall is mainly attributable to the rainfall type TfM and the rainfall type with local atmospheric moistening, water vapor convergence, and hydrometeor loss/convergence (tFM) in both schemes. The hydrometeor loss/convergence in TfM and tFM is caused by water clouds through rainfall and evaporation of rain and by ice clouds through the conversion to water hydrometeor to ice hydrometeor over raining stratiform regions, which is different from the dominance of ice microphysics in stratiform rainfall (Houghton 1968). The hydrometeor loss/convergence in TfM is primarily attributable to water clouds through rainfall and evaporation of rain over convective regions. The hydrometeor gain/divergence in TFm is caused by water clouds through the vapor condensation and by ice clouds through vapor deposition and the conversion from water hydrometeor to ice hydrometeor over convective regions. Like the stratiform rainfall in S07, the mixed rainfall mainly consists of the rainfall types TfM and tFM. The hydrometeor loss/convergence is attributable to water clouds through rainfall and the evaporation of rain, which is similar to the convective rainfall in S07.

Acknowledgement: The authors thank Dr. W.-K. Tao at NASA/GSFC for his cloud resolving model, Prof. M. Zhang at the State University of New York for his TOGA COARE forcing data.

REFERENCES:

[1] HOUGHTON H G. On precipitation mechanisms and their artificial modification [J]. J. Appl. Meteor., 1968, 7(5): 851-859.
[2] CHURCHILL D D, HOUZE R A Jr. Development and structure of winter monsoon cloud clusters on 10 December 1978 [J]. J. Atmos. Sci., 1984, 41: 933-960.
[3] STEINER M, HOUZE R A Jr. Three-dimensional validation at TRMM ground truth sites: Some early results from Darwin, Australia [C]// Preprints, 26th Int. Conf. On Radar Meteorology, Norman: Amer. Meteor. Soc., 1993: 417-420.
[4] ROSENFELD D, AMITAI E, WOLFF D B. Classification of rain regimes by the three-dimensional properties of reflectivity fields [J]. J. Appl. Meteor., 1995, 34(1): 198-211.
[5] STEINER M, HOUZE R A Jr, YUTER S E. Climatological characterization of three-dimensional storm structure from operational radar and rain gauge data [J]. J. Appl. Meteor., 1995, 34(9): 1978-2007.
[6] BIGGERSTAFF M I, LISTEMAA S A. An improved scheme for convective/stratiform echo classification using radar reflectivity [J]. J. Appl. Meteor., 2000, 39(12): 2129-2150.
[7] TAO W K, SIMPSON J. Modeling study of a tropical squall-type convective line [J]. J. Atmos. Sci., 1989, 46(2): 177-202.
[8] TAO Wei-kuo, LANG S, SIMPSON J, et al. Vertical profiles of latent heat release and their retrieval for TOGA COARE convective systems using a cloud resolving model, SSM/I, and ship-borne radar data [J]. J. Meteor. Soc. Japan, 2000, 78(4): 333-355.
[9] XU Kuan-man. Partitioning mass, heat, and moisture budgets of explicit simulated cumulus ensembles into convective and stratiform components [J]. J. Atmos. Sci., 1995, 52(1): 1-23.
[10] LANG S, TAO Wei-kuo, SIMPSON J, et al. Modeling of convective-stratiform precipitation processes: Sensitivity to partition methods [J]. J. Appl. Meteor., 2003, 42(4): 507-523.
[11] TAO Wei-kuo, SIMPSON J, SUI Chung-hsiung, et al. Heating, moisture and water budgets of tropical and midlatitude squall lines: Comparisons and sensitivity to longwave radiation [J]. J. Atmos. Sci., 1993, 50(5): 673-690.
[12] SUI Chung-hsiung, LAU Ka-ming, TAO Wei-kuo, et al.

The tropical water and energy cycles in a cumulus ensemble model. Part I: Equilibrium climate [J]. J. Atmos. Sci., 1994, 51(5): 711-728.
[13] CUI Xiao-peng, LI Xiao-fan. Role of surface evaporation in surface rainfall processes [J]. J. Geophys. Res. 2006, 111: D17112, doi:10.1029/2005JD006876.
[14] CUI Xiao-peng, Zhou Yu-shu, LI Xiao-fan. 2007: Cloud microphysical properties in tropical convective and stratiform regions [J]. Meteor. Atmos. Phys., 2007, 98(1): 1-11.
[15] PING Fan, LUO Zhe-xian, LI Xiao-fan. Microphysical and radiative effects of ice microphysics on tropical equilibrium states: A two-dimensional cloud-resolving modeling study [J]. Mon. Wea. Rev., 2007, 135(7): 2794-2802.
[16] XU Xiao-feng, XU Feng-wen, LI Bai. A cloud-resolving modeling study of a torrential rainfall event over China [J]. J. Geophys. Res., 2007, 112: D17204, doi: 10.1029/2006JD008275.
[17] GAO Shou-ting, LI Xiao-fan. Responses of tropical deep convective precipitation systems and their associated convective and stratiform regions to the large-scale forcing [J]. Quart. J. Roy. Meteor. Soc., 2008, 134(4): 2127-2141.
[18] PING F, LUO Zhe-xian. Microphysical and radiative effects of ice clouds on diurnal variations of tropical convective and stratiform rainfall [J]. Atmos. Res., 2009, 93(4): 862-873.
[19] ZHOU Yu-shu, LI Xiao-fan. Sensitivity of convective and stratiform rainfall to sea surface temperature [J]. Atmos. Res., 2009, 92(2): 212-219.
[20] WANG Yi, SHEN Xin-yong, LI Xiao-fan. Microphysical and radiative effects of ice clouds on responses of rainfall to the large-scale forcing during pre-summer heavy rainfall over southern China [J]. Atmos. Res., 2010, 97(1): 35-46.
[21] SUI Chung-hsiung, TSAY Ching-tung, LI Xiao-fan. Convective stratiform rainfall separation by cloud content [J]. J. Geophys. Res., 2007, 112: D14213, doi:10.1029/2006JD008082.
[22] CANIAUX G, REDELSPERGER J L, LAFORE J P. A numerical study of the stratiform region of a fast-moving squall line. Part I: General description and water and heat budgets [J]. J. Atmos. Sci., 1994, 51(16): 2046-2074.
[23] SHEN Xin-yong, WANG Yi, ZHANG Nan, et al. Precipitation and cloud statistics in the deep tropical convective regime [J]. J. Geophys. Res., 2010, 115: D24205, doi: 10.1029/2010JD014481.
[24] GAO Shou-ting, CUI Xiao-peng, ZHOU Yu-zhu, et al. Surface rainfall processes as simulated in a cloud resolving model [J]. J. Geophys. Res., 2005, 110, D10202, doi:10.1029/2004JD005467.
[25] SOONG S T, OGURA Y. Response of tradewind cumuli to large-scale processes [J]. J. Atmos. Sci., 1980, 37(9): 2035-2050.
[26] SOONG S T, TAO Wei-kuo. Response of deep tropical cumulus clouds to mesoscale processes [J]. J. Atmos. Sci., 1980, 37(9): 2016-2034.
[27] TAO Wei-kuo, SIMPSON J. The Goddard Cumulus Ensemble model. Part I: Model description [J]. Terr. Atmos. Oceanic Sci., 1993 4(1): 35-72.
[28] LI X, SUI Chung-hsiung, LAU Ka-ming. Radiative-convective processes in simulated diurnal variations of tropical oceanic convection [J]. J. Atmos. Sci., 1998, 55(13): 2345-2359.
[29] LI X, SUI Chung-hsiung, LAU Ka-ming, et al. Large-scale forcing and cloud-radiation interaction in the tropical deep convective regime [J]. J. Atmos. Sci., 1999, 56(17): 3028-3042.
[30] LI X, SUI Chung-hsiung, LAU Ka-ming. Dominant cloud microphysical processes in a tropical oceanic convective system: A 2-D cloud resolving modeling study [J]. Mon. Wea. Rev., 2002, 130(10): 2481-2491.
[31] RUTLEDGE S A, HOBBS P A. The mesoscale and microscale structure and organization of clouds and precipitation in midlatitude cyclones. Part VIII: A model for the "seeder-feeder" process in warm-frontal rainbands [J]. J. Atmos. Sci., 1983, 40(8): 1185-1206.
[32] RUTLEDGE S A, HOBBS P A. The mesoscale and microscale structure and organization of clouds and precipitation in midlatitude cyclones. Part XII: A diagnostic modeling study of precipitation development in narrow cold-frontal rainbands [J]. J. Atmos. Sci., 1984, 41(20): 2949-2972.
[33] LIN Yuh-lang, FARLEY R D, ORVILLE H D. Bulk parameterization of the snow field in a cloud model [J]. J. Climate Appl. Meteor., 1983, 22(6): 1065-1092.
[34] TAO Wei-kuo, SIMPSON J, MCCUMBER M. An ice-water saturation adjustment [J]. Mon. Wea. Rev., 1989, 117(1): 231-235.
[35] KRUEGER S K, FU Qiang, LIOU Kuo-nan, et al. Improvement of an ice-phase microphysics parameterization for use in numerical simulations of tropical convection [J]. J. Appl. Meteor., 1995, 34(1): 281-287.
[36] CHOU Ming-dah, KRATE D P, RIDGWAY W. Infrared radiation parameterization in numerical climate models [J]. J. Climate, 1991, 4(4): 424-437.
[37] CHOU Ming-dah, SUAREZ M J, HO Chang-hoi, et al. Parameterizations for cloud overlapping and shortwave single scattering properties for use in general circulation and cloud ensemble models [J]. J. Climate., 1998, 11(2): 201-214.
[38] CHOU Ming-dah, SUAREZ M J. An efficient thermal infrared radiation parameterization for use in general circulation model [R]// NASA Tech. Memo., Greenbelt: NASA/Goddard Space Flight Center, 104606, 1994, Vol. 3, 85pp.
[39] ZHANG Ming-hua, LIN Jia-lin. Constrained variational analysis of sounding data based on column-integrated budgets of mass, heat, moisture, and momentum: Approach and application to ARM measurements [J]. J. Atmos. Sci., 1997, 54(11): 1503-1524.
[40] WELLER R A, ANDERSON S P. Surface meteorology and air-sea fluxes in the western equatorial Pacific warm pool during TOGA COARE [J]. J. Climate, 1996, 9(7): 1959-1990.
[41] GAO Shou-ting, LI X. Cloud-resolving modeling of convective processes [M]. Amsterdam: Springer, 2008: 206pp.
[42] SUI Chung-hsiung, Li X. A tendency of cloud ratio associated with the development of tropical water and ice clouds [J]. Terr. Atmos. Ocean. Sci., 2005, 16(2): 419-434.

Citation: SHEN Xin-yong, LIU Jia and Xiaofan LI. Evaluation of convective-stratiform rainfall separation schemes by precipitation and cloud statistics. *J. Trop. Meteor.*, 2012, 18(1): 98-107.